Single-domain crystal-anisotropy-dominated coercivity

D. I. Paul
Physics Department, Portland State University, Portland, Oregon 97207

A. Cresswell
Physics Department, Shippensburg University, Shippensburg, Pennsylvania 17257
(Received 21 August 1992; revised manuscript received 22 March 1993)

We present a theoretical approach to the problem associated with the anomalous coercivity observed in granular magnetic solids such as iron or cobalt embedded in an insulating medium and to amorphous multilayer thin films. In this paper we show that if the magnetic moments at the granular surface or multilayer interface are pinned, such enhanced coercivity is predictable. The model used assumes a one-dimensional dependence of the magnetization (along the length of the granule or the depth of the layer). That dimension is taken to be small to inhibit the appearance of domain walls parallel to that direction. We consider materials whose energy is dominated by a Zeeman term, an anisotropy term, a demagnetization term, and an exchange term. The exchange term is determined with the use of the Landau semiclassical approximation, and thus we do away with the mean-field approximation. The coercivity is defined in such a manner as to retain its nonreversible nature. Results are presented in dimensionless units. When applied to cobalt and iron, they give values in accordance with experimental data.

I. INTRODUCTION

A good deal of attention has been given to the magnetic properties of small metal granules embedded in an immiscible medium which may be insulating,[1,2] such as iron and cobalt in SiO_2, Al_2O_3, HgO, etc., or an oxidizing layer,[3] or simply isolated granules using such methods as gas evaporation.[4] At sizes and packing fractions sufficiently small to exhibit single-domain behavior and isolation of one granule from the other, the medium shows anomalous magnetic behavior. In particular, for those granules still large enough to be ferromagnetic rather than superparamagnetic, coercivities considerably in excess of the zero-temperature rotational coercivity due to crystal anisotropy, (i.e., 2K/M), are observed. Demagnetization effects provided by such geometries as chain of spheres or large aspect ratios[1] could possibly account for these values, but such geometries are not observed. Micromagnetic calculations[5] and further experimental studies[6] on passivated γ-Fe_2O_3 particles have shown that the thickness and magnetic state of the surrounding oxide layer affects the coercivity.

The original problem of single-domain particles was theoretically considered[7] some 40 years ago using a much simplified approach for the effects of crystal anisotropy—simply equating the maximum coercivity field to the ratio of twice the anisotropy constant to the magnetization—no consideration being given to the variation of the magnetic-moment angle θ along the path in real space and the effect of the exchange energy. Since then a good deal of excellent work has been done on this problem using numerical procedures for particle sizes in the range 100–500 A in three dimension (see Ref. 5 and references given therein).

In this paper, we show that, when the surface atoms of these particles have their magnetization pinned—either through surface stress or some form of exchange coupling to the strongly bonding insulating matrix, such enhanced coercivity is predictable. Further, our model applies equally well to amorphous ferromagnetic thin films whose interfaces are also pinned through stress or exchange coupling.

In particular, assuming a one-dimensional spatial dependence, we have computed the angular distribution along the path of the magnetization in the presence of a reverse external magnetic field, where the surface magnetic moments are pinned and parallel to each other. We assume the absence of domain walls in the granular solid (implying a short diameter), and that the domain walls do not play a dominant role in the reversal process in thin films due to their amorphicity. Demagnetization effects are discussed later in this paper. Initially, we assume that the magnetization is dominated by crystal anisotropy and exchange.

The coercivity is calculated without the assumption of mean-field theory. (Calculations using mean-field theory can be found in Refs. 8–10.) It is defined as that value of the external magnetic field wherein one of the Lagrange-Euler minimal energy paths, whose net magnetization has a component antiparallel to the external magnetic field, disappears; thus causing an avalanche rotation of the magnetic moments into a second Lagrange-Euler energy path after dissipating the available energy. The net component of magnetization now lies parallel to the external field.

The avalanche of moments being essentially nonreversible, the nature of coercivity is preserved. The external field triggering that sudden change of configuration is, however, arrived in a reversible fashion, assuring the conservation of energy and the applicability of the Euler Lagrange equations. For this model to be valid, we must consider materials whose relaxation times are long

0163-1829/93/48(6)/3803(7)/$06.00

enough to allow the avalanche to take place (which is certainly not a constraining assumption at low temperatures).

II. MODEL

We consider a ferromagnetic material bounded by the length L along the X axis in the presence of an external uniform magnetic field in the negative Z direction (see Fig. 1). The magnetization within the material is assumed to vary as a function of X only—thus simplifying the problem—and is free to rotate in the YZ plane, the angle of rotation θ being measured from the Z axis (see Fig. 1). In order to describe a typical situation, the material is assumed to possess an anisotropy field in the YZ plane at an angle Θ of 45° with the Z axis. This choice of angle is used strictly as an illustrative example—it being an average value. (In a further section of this paper, we also consider different anisotropy angles.)

We assume that the magnetic moments at the ends or surface of the material ($X=0$ and L) are rigidly pinned such that they point in the $+Z$ direction. This assumption of surface pinning follows the ideas given by Chien and co-workers[1,2] and others in which they point out that for example, "in the granular Fe-SiO_2 systems the particles are strongly bonded to the insulating matrix and may be subject to very large stresses" and that "the metal-insulator interface may dominate the coercivity of such systems." Similarly, surface exchange pinning may also result.

We also assume that the length L is sufficiently small so that domain walls are prohibited. The exchange field is utilized in the semiclassical form originally proposed by Landau. Thus, we are effectively considering the coercivity due to crystal anisotropy, demagnetization and exchange energy of single-domain particles including correlations.

We first investigate the dynamics of the magnetization process for this model and consider only exchange, anisotropy, and Zeeman energies. Further, we assume long wavelengths (thus placing us in the field of micromagnetics). However, we do not restrict ourselves to the mean-field approximation. Demagnetization terms are initially neglected (we comment further on this later) as is the component of the magnetization perpendicular to the YZ plane.

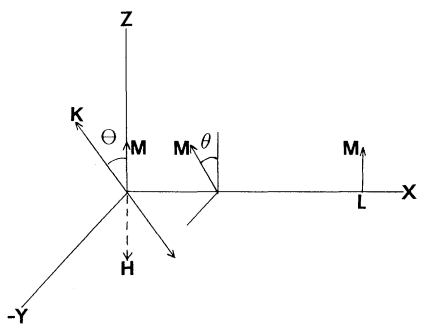

FIG. 1. Diagram of the magnetization m over sample length L. The angle θ is assumed to be a function of X only and in the YZ plane with θ_m at $X=L/2$ being, by symmetry, an extremal value. The anisotropy K is also in the YZ plane at an angle Θ with respect to the Z axis, while the external magnetic field H is parallel to the Z axis.

We note that the symmetry imposed implies that the direction of magnetization at the midpoint, $X=L/2$, is an extremum. We shall assume that the material is initially magnetically saturated in the $+Z$ direction. The external magnetic field is then reversed such that it points in a direction opposite to this magnetization (in the $-Z$ direction). Because of our boundary conditions and the aforementioned symmetry, it suffices to consider only the region ($0\le X\le L/2$) wherein θ varies from 0 degrees at $X=0$ to θ_m at $X=L/2$, where θ_m represents an extremum value—in this case a maximum.

Our energy over this region is taken as

$$E=2\int_0^{L/2}[A(d\theta/dX)^2+K\sin^2(\theta-\Theta)-HM\cos\theta]dX\ , \tag{1}$$

where E is the energy per unit area perpendicular to the length L. The extremum energy path, determined by the Lagrange-Euler equation derived from (1), is

$$-2A(d^2\theta/dX^2)+K\sin2(\theta-\Theta)+MH\sin\theta=0\ . \tag{2}$$

A first integral is easily obtained which, upon imposing the boundary condition above, ($\theta=\theta_m$ and $d\theta/dX=0$ at $X=L/2$) yields the equation

$$(K/2A)^{1/2}\int_0^{L/2}dX=\int_0^{\theta_m}[\cos2(\theta_m-\Theta)-\cos2(\theta-\Theta)+h(\cos\theta_m-\cos\theta)]^{-1/2}d\theta\ , \tag{3}$$

where $h=2HM/K$, the ratio of twice the magnetostatic energy constants to the anisotropy constant. Since the anisotropy angle Θ was assumed to be 45°, we get for the Lagrange-Euler path the expression

$$I=\int_0^{\theta_m}[\sin2\theta_m-\sin2\theta+h(\cos\theta_m-\cos\theta)]^{-1/2}d\theta\ , \tag{4}$$

where $I=L/L_0$, and $L_0=(8A/K)^{1/2}$ is a function of the material characteristics only. We recognize the factor L_0 as about equal to a wall width, $\pi\delta$, where $\delta=(A/K)^{1/2}$. However, since our surface magnetic moments are pinned and parallel to each other, we may consider lengths L which are several times L_0, i.e., $L/L_0<5$, and still maintain our assumption of the absence of domain walls. Inasmuch as, for a given material, L/L_0 has a fixed value, we recognize that the existence of a Lagrange-Euler path is dependent on the values of the two parameters, h and θ_m, in the integral.

We are interested in determining the dynamic coercivity for this model as a prelude to subsequent investigations of the response of more realistic materials. Thus, we have evaluated the integral for negative values of h.

III. RESULTS

The various behaviors of the materials under consideration can be understood from studying Fig. 2, which

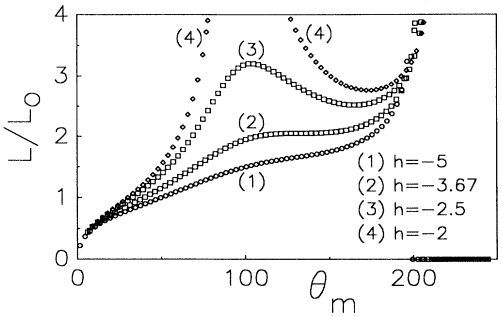

FIG. 2. Value of the dimensionless sample length L/L_0 vs θ_m, the maximum angle of magnetization in degrees along the Lagrange-Euler path for several values of the dimensionless external magnetic field, $h=2HM/K$. The anisotropy angle is 45°. Note the undefined values (shown as zeros) for all h in the range $\theta_m >$ about 210° and in the approximate range 67°–143° for $h<-2$.

shows the relationship between the dimensionless distance parameter $I(=L/L_0)$ and the maximum angle θ_m reached by the moments at the distance, $L=L_0/2$, from the pinned ends. Thus, each θ_m corresponds to a unique and well defined configuration of moments characterized by their corresponding distance parameter I.

Let us start by making two general remarks on the results exhibited by Fig. 2. First, we note that there exists regions of forbidden θ_m's (corresponding to values of θ_m leading to negative square roots in the distance integral). For $0>h>-2$, there exists two such regions—one for large θ_m ($\theta_m >$ about 240°)—and an additional region with θ_m centered at about 100°. As h increases from zero in the negative Z direction to exactly -2, this additional forbidden range of θ_m is narrowed down to a point. As h increases negatively past -2, this forbidden region of θ_m's yields to a local maximum, which in turn disappears completely at the critical field $h_c=-3.67$ (corresponding to $I_c=2.05$ at $\theta_m=133°$), and leaves I as a monotonically increasing function of θ_m. Increasing h past this value does not change the general shape of the plot. Second, we see that materials of an arbitrarily large distance parameter will always have at least one stable configuration θ_m, since the integral in Eq. (4) can be made arbitrarily large by choosing θ_m close enough to singularities of the integral. For $0>h>-2$, there are three such singularities; for $h<-2$ there is always one.

We can now distinguish, according to the distance parameter, two different types of behavior when the material is subject to field reversal.

(1) Materials with distance parameters $I<I_c$: For a material of this type, the configuration specified by θ_m is unique for any given arbitrary h. Thus, there exists a unique Lagrange-Euler path of angles from zero to θ_m which minimizes the energy at a given h. In other words, I versus θ_m is a single-valued function for any h as long as $I<I_c$. As h increases negatively, θ_m also increases—moving continuously through the upper half space into the lower half space.

(2) Materials with distance parameters $I>I_c$: For these materials, Fig. 2 shows that the number of possible configurations depends on the value of the external field parameter h. For h small enough (e.g., negative h less than 2.5 for a material whose $I=3.2$), there exist three Lagrange-Euler configurations that optimize the energy; these correspond to three maximum angles θ_{m1}, θ_{m2}, and θ_{m3} (where $\theta_{m1}<\theta_{m2}<\theta_{m3}$). Of these, however, only θ_{m1} and θ_{m3} minimize the energy. (θ_{m2} maximizes the energy.) As h increases negatively, two of the configurations disappear suddenly leaving only θ_{m3} as an allowed configuration (e.g., the disappearance occurs at $h=-2.5$ for a material whose $I=3.2$). The quantity θ_{m3} increases as h increases negatively.

We have also computed the energy as a function of configuration for a series of external fields. The results are presented in Fig. 3 and show well the evolution of the minima introduced above. We note that the minimal path denoted by θ_{m3} (whose net Z component of magnetization lies in the negative Z direction) has a smaller energy per unit length than θ_{m1} except for that situation in which θ_{m3} becomes unobtainable due to I being very small. Just prior to I reaching this value, the energy corresponding to θ_{m3} is greater than that for θ_{m1}. Figure 4 shows the rapid rise of θ as a function of distance X for those paths corresponding to θ_{m3}, (i.e., $\theta_m=190°$). The value $\theta_m=135°$ corresponds on the average to zero net magnetization.

IV. ANALYSES

The results described above for Figs. 2–4 suggest that the response of materials described by our model and subject to reverse or alternating fields, is critically dependent on the value of their distance parameter I. Moreover, the behavior described above suggests, as we shall now see, natural definitions for coercivity and switching fields.

A. Coercivity for materials with $I>I_c$

Starting from a saturation by a strong field initially in the positive Z direction, let us consider what happens when that field is turned off and then made to increase in

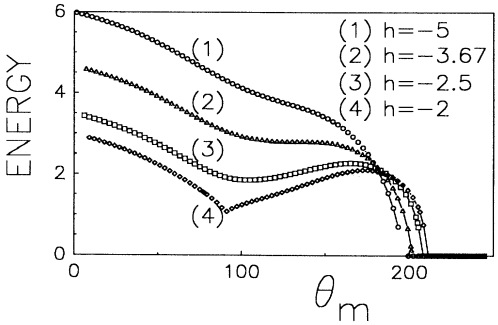

FIG. 3. Value of the energy per unit length ϵ in dimensionless units over the Lagrange-Euler path as a function of θ_m in degrees for the same values of h as in Fig. 2 [Note: $\epsilon=(E/\sqrt{2KA})/(L/L_0)$].

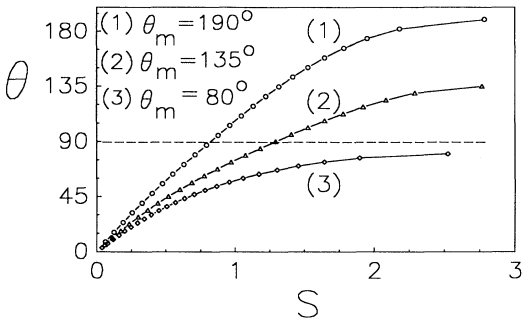

FIG. 4. θ in degrees as a function of position S over the Lagrange-Euler path for several values of θ_m. The dimensionless external field $h=-2.5$ and the anisotropy angle is 45°. We have marked the value $\theta=90°$ by a dashed line to indicate those magnetic moments having components in the lower half plane.

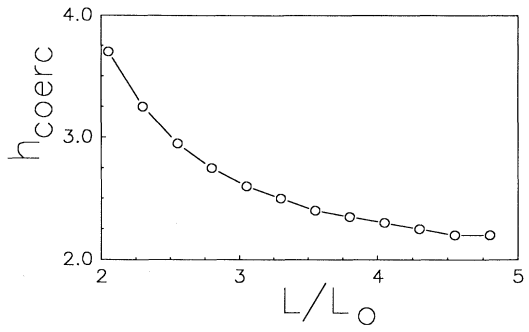

FIG. 5. Plot of dimensionless coercivity h_{COERC} as a function of reduced sample length L/L_0 at $\Theta=45°$.

the negative Z direction. For h still small (but now pointing in the negative Z direction) the moments occupy a configuration defined by θ_{m1} corresponding to a net positive magnetization (see, e.g., $h=-2.5$, $\theta_m=80°$ in Fig. 4). As the field increases in the negative Z direction, the moments stay trapped initially in the θ_{m1} configuration, while it remains a secondary minimum of energy. Coincidently, the energy minimum of the θ_{m3} configuration deepens. However, as a critical field called h_{COERC} is reached, θ_{m1} and θ_{m2} coalesce and the associated configuration minimum and maximum disappear. Since θ_{m1} is no longer a valid maximum angle of a stable configuration, the moments are forced to rotate to the lower hemisphere in a nonreversible fashion. The value of h_{COERC} is determined uniquely by the value I of the distance parameter for the given material (in the case of $I=3.2$ the critical field is given in Fig. 2 by $h_{\mathrm{COERC}}=-2.5$). Any further increase of h past h_{COERC} forces the moments to rotate further into the lower hemisphere as is manifested by an increasing θ_{m3}.

Depending on the material, the energy thus released could overcome the surface pinning, leading to an equilibrium configuration in the lower hemisphere, opposite from the initial configuration, with moments pinned along $-Z$. In this case the symmetry of the problem would clearly yield a symmetrical hysteresis loop. If the energy available is not sufficient to overcome the pinning, then the moments simply rotate (still in a nonreversible way, of course) to the θ_{m3} configuration leading to a nonsymmetrical hysteresis for this particular set of boundary conditions. However, we should point out that, in actual physical situations where pinning at the surface is caused by stresses, etc., there are granules with surfaces pins pinned "up" and there are granules with surface spins pinned "down," and therefore, on the average, the hysteresis loop is symmetrical. Thus, except in special circumstances, we should not expect to see this asymmetrical phenomenon. This is true even for a single granule where there may be a distribution of the directions of magnetic-moment pinning on the surface depending on the particular mechanism.

In light of either behavior, it is thus natural to define h_{COERC} as the coercivity of the material. Figure 5 presents a plot of the value of h_{COERC} as a function of the distance parameter I or L/L_0. With increasing distance parameter the moments have more room to rotate against the exchange and thus h_{COERC} is a decreasing function of length. (However, we restrict the magnitude of L/L_0 in order to maintain our assumption of no domain walls.)

B. Switching behavior for materials with $I < I_c$

For this range of distance parameters, the combination of pinned moments at the surface and short distances prevents the existence of two minima. As the h field is decreased from a positive value to zero and then increased in the negative z direction, θ_{m1} remains a stable configuration and increases continuously eventually bringing the average magnetization of the material towards the negative Z axis. We define the switching field h_{sw} as the field necessary to bring θ_{m1} to a value of 135°, which will, on the average, bring the magnetization of the material back to zero. Assuming that the end moments stay pinned, the process is reversible and the "hysteresis" curve has a vanishing enclosed area. This behavior justifies calling h_{sw} a switching field rather than a coercive field.

Figure 6 provides a plot of the switching fields versus the distance parameter. We have not gone below $L/L_0 \sim 0.7$ to avoid the superparamagnetic region. As before, increasing distances give the material more room to overcome the exchange, and thus h_{sw} is a decreasing function of length. (One should remark that a coercive

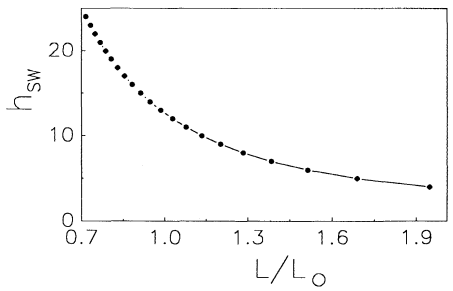

FIG. 6. Plot of dimensionless switching field h_{sw} as a function of dimensionless sample length L/L_0 at $\Theta=45°$.

behavior of materials with distance parameters in this range could be achieved by assuming a breakdown of the surface pinning of the moments.)

V. OTHER ANISOTROPY ANGLES

We have also considered the variation of the coercivity as a function of the anisotropy angle, Θ. In addition to its instructive value, such considerations are important for a granular system where there are many granules with different orientations and therefore many different anisotropy values. Also, it gives a sense of what is entailed in an amorphous material and gives some insight into the three-dimensional problem.

Thus, we have used Eq. (3) to obtain curves for the dimensionless coercivity h_{COERC} as a function of reduced path length similar to that given in Fig. 5 for $\Theta=45°$. Figure 7 is a graph of these curves for anisotropy angles 15°, 30°, 45°, and 60°. We see a considerable variation of coercivity, generally increasing as the anisotropy angle deviates in either direction from 45°. Also, we note the strong dependence on the normalized length, L/L_0.

To illustrate further the dependence on the anisotropy angle, we have graphed in Fig. 8 the critical length l_c as a function of the anisotropy angle. We remember from a previous section of this paper that l_c is that length such that for all $l<l_c$ there exists only one minimal energy path—thus yielding a continuous reversible switching type behavior rather than the coercive behavior associated with hysteresis loops and energy dissipation. We note that our curve separates the space into two regions. As the anisotropy angle approaches 0°, i.e., as the anisotropy direction becomes parallel to the direction of the applied external field and that of the pinned magnetic moments at the surface, l_c becomes very small and the coercivity mechanism dominates for practically all lengths. The reverse situation occurs as the anisotropy angle approaches 90°. Thus, in a sense this curve represents a "phase transition" re: hysteresis. Of course, one must apply caveats to our result such as that the surface moments remain pinned during the reversal process, that there are no material inhomogeneities nor acoustic emission to yield energy dissipation, etc.

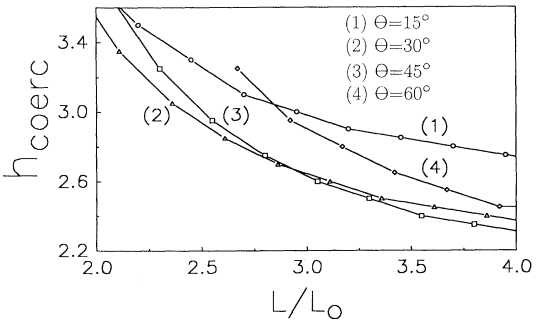

FIG. 7. Plot of dimensionless coercivity h_{COERC} as a function of reduced sample length for anisotropy angles 15°, 30°, 45°, and 60°.

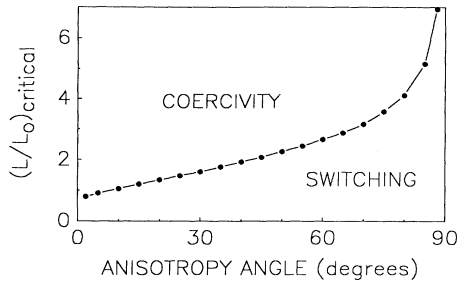

FIG. 8. Plot of the critical sample length $(L/L_0)_{\mathrm{CRITICAL}}$ as a function of the anisotropy angle. The two regions of different magnetic reversal mechanism, coercivity and switching, are shown.

VI. DEMAGNETIZATION ENERGY

Before discussing applications of these normalized coercive and switching fields to actual materials, we would like to comment on the demagnetization energy in granular solids where the granule can be thought of as something between a sphere and a cube—the essential point being that the dimensions of the granule are about the same in all directions. Then, in a one-dimensional functional relationship for the magnetization, the demagnetization energy can be represented by a simple localized magnetostatic energy of the form

$$E_{\mathrm{demag}}=4\pi NM^2\sin^2\theta\ . \tag{5}$$

(For clarity in visualization, one can think of θ as now being in the XZ plane. In either case, Eq. (1) remains the same.) The resultant equation equivalent to Eq. (3) is

$$(K'/2A)^{1/2}\int_0^{L/2}dx=\int_0^{\theta_m}[\cos2(\theta_m-\Theta')-\cos2(\theta-\Theta')+h'(\cos\theta_m-\cos\theta)]^{-1/2}d\theta\ , \tag{6}$$

where

$$K'=[(4\pi NM^2+K\cos2\Theta)^2+K^2\sin^2 2\Theta]^{1/2}\ . \tag{7a}$$

$h'=2HM/K'$, and Θ' is defined such that

$$\sin2\Theta'=(K\sin2\Theta)/K'$$

and

$$\cos2\Theta'=(4\pi NM^2+K\cos2\Theta)/K'\ . \tag{7b}$$

If we now take $\Theta'=45°$, where Θ is then determined as a function of K and $4\pi NM^2$, then our equation would be identical to Eq. (4) with K' and h' substituted for K and h. Of course, for specific values of K, N, and Θ, this may not be a reasonable choice. But what this does show is that, even in the presence of large demagnetization effects, our results should remain qualitatively correct.

We note here that we could have done a three-dimensional calculation for the sphere including temperature variation— using mean-field theory for the exchange Hamiltonian. However, mean-field theory tends to falsely mask the effect of spin correlations and thus fluctuations, while, at the same time, giving an artificial dependence of the coercivity on the exchange energy.[11] Although valid for the coercivity in some cases, the mean-field approximation would clearly be in contradiction with the geometry of our problem (the average magnetization not staying parallel to the Z axis).

VII. APPLICATION TO IRON AND COBALT

When the results of the previous section are applied to iron and cobalt, we obtain Figs. 9(a) and 9(b) for iron and Fig. 9(c) for cobalt. Although the customary maximum diameter of a single-domain sphere is usually given as a little less than the size of a domain-wall width, we would emphasize here that our boundary conditions of fixed magnetic moments at the surface of our material preclude the existence of domain walls at lengths substantially larger—a factor of 4 to 5 not being excessive. With respect to a lower bound, superparamagnetism begins to appear at about $L < 180$ A (Ref. 5). Our calculations being done at $T=0$ K, we do not consider superparamagnetism in our model, and one must be careful with the interpretation of our work for lengths less than this value.

Our results for iron show a coercivity of the same order of magnitude as those observed by Chien and others (Refs. 1–4). For a length of 1600 A we obtain a coercivity of ~400 Oe and for a length of 2500 A, the coercivity is ~325 Oe. At smaller lengths, we are in the switching field regime. For iron at $L=1100$ A, the switching field is ~590 Oe, while at $L=400$ A, the switching field increases to ~3500 Oe. The coercivity of cobalt is much higher. For a length of 900 A, the coercivity is ~3900 Oe, while at $L=300$ A the switching field is ~11 000 Oe.

Physically, the reason these values are so much higher than the crystal-anisotropy field can be traced to the resistance of the exchange energy to angular variations of the magnetic moment along the length L of the material—resulting from the fixed direction of the pinned magnetic moment at the surface. Admittedly, this is a model based on a one-dimensional spatial dependence. We can only assume that a two-dimensional pinned spherical surface would give a more quantitatively correct match between theory and experiment. Furthermore, we have assumed that the direction of the magnetic moments at the surface are rigidly fixed—perhaps an overemphasis of the actual physical condition.

Further, we must consider the experimental dependence of the coercivity on the size of the granules. These experiments show an increase in $Fe_{75}(SiO_2)_{25}$ at 42 vol. % iron from 1500 to 3000 Oe as the substrate temperatures is increased from about 300 to 800 and then a rapid drop beyond this.[1,2] We attribute the initial increase to the change from superparamagnetism to ferromagnetism— or, to place it in context with our work, we attribute our continued rise in coercivity, as the length continues to decrease to the fact that our model does not contain the effect of temperature fluctuations—our calculations being done at 0 K.

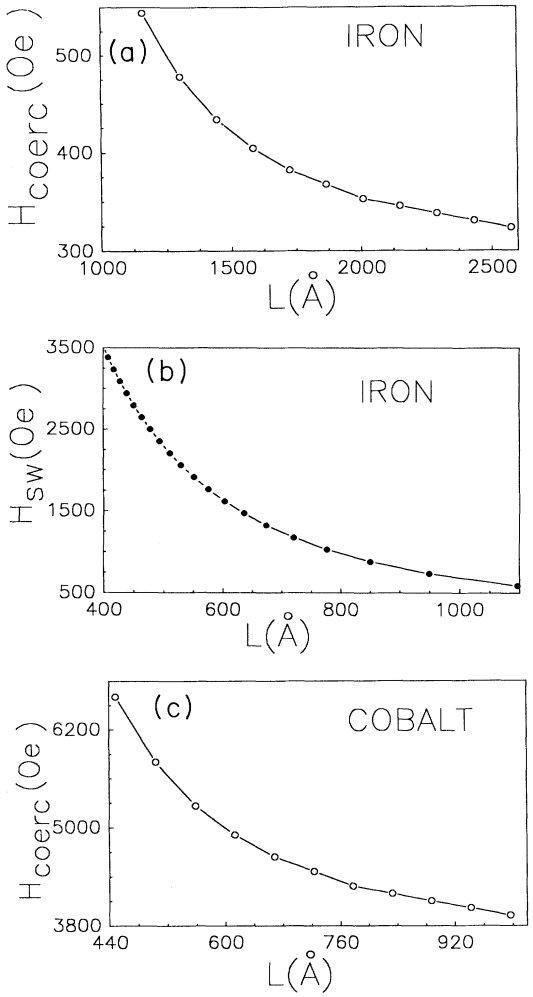

FIG. 9. (a) Example of coercivity vs sample length for iron. We have taken $A=2\times10^{-6}$ ergs/cm, $K=5\times10^{5}$ ergs/cm^3, $M=1700$, and $\Theta=45°$. (b) Example of switching field vs sample length for iron using same values as in Fig. 9(a). (c) Example of coercivity vs sample length for cobalt. We have taken $A=3\times10^{-6}$ ergs/cm, $K=5\times10^{5}$ ergs/cm^3, $M=1400$, and $\Theta=45°$.

The difference in our results compared to those of Schabes and Bertram[5] is of course attributable to our restriction to a one-dimensional functional dependence and thus the absence of multidimensional demagnetization effects such as flower states, etc. Another major factor is the difference in boundary conditions. We have assumed that stresses and exchange fields have pinned our surface states such that their directions of magnetization are fixed. The validity of this assumption depends strongly on the experimental design of the ferromagnetic material. In many cases, it is close to the truth. Thus, we feel that the physical insight obtainable under these assumptions makes these results of considerable interest.

[1]C. L. Chien, J. Appl. Phys. **69**, 5267 (1991).
[2]G. Xiao and C. L. Chien, J. Appl. Phys. **63**, 4253 (1988).
[3]S. Gangopadhyay, G. C. Hadjipanayis, S. I. Shah, C. M. Sorensen, K. J. Klabunde, V. Papaefthymiou, and A. Kostikas, J. Appl. Phys. **70**, 5888 (1991).
[4]W. Gong, H. Li, Z. Zhao, and J. Chen, J. Appl. Phys. **69**, 5119 (1991).
[5]M. E. Schabes and H. Neal Bertram, J. Appl. Phys. **67**, 5149 (1990).
[6]T. Miyahara and K. Kawakami, IEEE Trans. Magn. **23**, 2877 (1987).
[7]C. Kittel, Phys. Rev. **70**, 965 (1946); W. F. Brown, J. Appl. Phys. **30**, 130S (1959); L. Néel, C. R. Seances Soc. Biol. Paris **224**, 1488 (1947).
[8]A. Cresswell and D. I. Paul, J. Appl. Phys. **67**, 398 (1990); **67**, 5775 (1990).
[9]E. Callen, J. J. Liu, and J. R. Cullen, Phys. Rev. B **16**, 263 (1977).
[10]J. D. Patterson, G. R. Gruzalski, and D. J. Sellmyer, Phys. Rev. B **18**, 1377 (1978).
[11]D. I. Paul and L. M. Pecora, Phys. Rev. B **19**, 4608 (1979).